

# Flow Energy Piezoelectric Bimorph Nozzle Harvester

Stewart Sherrit, Hyeong Jae Lee, Phillip Walkemeyer, Jennifer Hasenoehrl,  
Jeffery L. Hall,

**Jet Propulsion Laboratory, California Institute of Technology, Pasadena, CA**

Tim Colonius, Luis Phillipe Tosi

**California Institute of Technology, Pasadena, CA**

Alvaro Arrazola, Namhyo Kim, Kai Sun, Gary Corbett

**Chevron Corporation, Houston, TX**

**Abstract** – There is a need for a long-life power generation scheme that could be used downhole in an oil well to produce 1 Watt average power. There are a variety of existing or proposed energy harvesting schemes that could be used in this environment but each of these has its own limitations. The vibrating piezoelectric structure is in principle capable of operating for very long lifetimes (decades) thereby possibly overcoming a principle limitation of existing technology based on rotating turbo-machinery. In order to determine the feasibility of using piezoelectrics to produce suitable flow energy harvesting, we surveyed experimentally a variety of nozzle configurations that could be used to excite a vibrating piezoelectric structure in such a way as to enable conversion of flow energy into useful amounts of electrical power. These included reed structures, spring mass-structures, drag and lift bluff bodies and a variety of nozzles with varying flow profiles. Although not an exhaustive survey we identified a spline nozzle/piezoelectric bimorph system that experimentally produced up to 3.4 mW per bimorph. This paper will discuss these results and present our initial analyses of the device using dimensional analysis and constitutive electromechanical modeling. The analysis suggests that an order-of-magnitude improvement in power generation from the current design is possible.

**Keywords:** Actuators, Piezoelectric Devices, Flow Energy Harvesting, bimorphs, transducers

## I. Introduction

There are several energy sources in the environment such as light, thermal, flow, and mechanical vibration that can be tapped to provide useful energy. The conversion of these ubiquitous energy sources into useful amounts of electrical energy is called energy harvesting. In this paper we are investigating using fluid flow to induce vibrations in piezoelectric transducers to generate electricity. A variety of energy harvesting systems have been developed using piezoelectric or electrostrictive materials and many distinct vibration modes have been used to generate electrical power[ 1]. The energy harvesting application we are targeting is in downhole oil/water flow with the potential for the ambient pressures to reach 30000 psi and a temperature up to 200 °C. The necessity for energy harvesting in downhole oil producing wells is crucial as transmitting power from the surface is complicated by difficulty of making electrical connections across production packers. If the power can be produced locally by energy harvesting of the oil flow, the need to transmit power down the hole is removed, and downhole devices can be powered locally which reduces the overall complexity and difficulty of the system.

The approach we are investigating to harvest power is to use flow energy from the oil/water flow in downhole pipes; for example, oil can flow as fast as 15 m/s in the inner pipe, and the mechanical power associated with this high flow rate can be calculated as follows:

$$P = \frac{E}{t} = \frac{1}{2} \rho A v^3 = \frac{\rho Q^3}{2A^2} \quad (1)$$

where E is the kinetic energy, t is the time,  $\rho$  is the density, A is the cross sectional area of the pipe, v is the fluid velocity and Q is the flow rate ( $Q=v/A$ ). Ignoring any fluid compression effects at 15 m/s and a density of 900 kg/m<sup>3</sup> of oil in a 4 inch diameter pipe, we have 12.5 kW of power flowing across the cross sectional area of the pipe. Since the power is proportional to the cube of the velocity one can extract 3%

of the total power and only reduce the velocity by 1%. This suggests that one can easily extract useful power of the order of 10 watts without noticeably impeding the flow rate. This power may then be conditioned and used to do useful work downhole.

The mechanical energy can be converted into electrical energy through various transduction mechanisms, such as piezoelectric, electromagnetic and electrostatic[1]. Among them, piezoelectrics have been the mainstay for energy harvesting system due to their high electromechanical coupling with no external voltage source requirement [2,3,4,5,6,7,8,9,10,11]. In addition, they can operate with limited strain and in non rotating systems which offers the potential to produce long life harvesting systems due to limited wear, and piezoelectric materials with large piezoelectric activity and with Curie temperatures in the 300 °C range are commercially available so the potential to operate at higher temperatures is also an advantage. A variety of studies have looked at methods to convert flow energy into vibrations including vortex shedding[12,13,14,15,16], flapping motions[17] and hydraulic pressure[18]. This paper presents the results of our experiments on a variety of designs for flow energy harvesters which used nozzles and/or flow cavities along a pipe to produce conditions that excite a vibrating piezoelectric structure. The performance and generated average power of each nozzle investigated will be presented in this paper.

## II. Electromechanical model of a piezoelectric cantilever

A cantilevered beam with one or two piezoelectric layers (a unimorph or a bimorph) has been used to design our energy harvesting devices. The key benefit of this design is it allows the piezoelectric transducer to have a low resonant frequency, allowing the cantilever system to match the frequency content of the unsteady flow. This design also offers large amplitude of vibration for a given oscillatory force (i.e., fluid flow), increasing the mechanical power stored in the cantilever system. Figure 1 shows a schematic diagram of parallel bimorph, where the two piezoelectric layers have the same polarization directions, and the electric voltage is applied between the intermediate electrode and the top/bottom electrodes. The constitutive equations describing the behavior of the cantilever type piezoelectric bimorph were derived by Smits et al.[19,20], where the slope,  $\alpha$  and the deflection,  $\delta$  at the end, the displaced volume,  $v$  and the charge on the electrode,  $Q$  is related to a moment at the end,  $M$ , a force at the end,  $F$ , a uniformly applied pressure,  $p$  and the voltage over the electrodes,  $V$  through a bimorph matrix. The matrix under static condition can be written by the following equation:

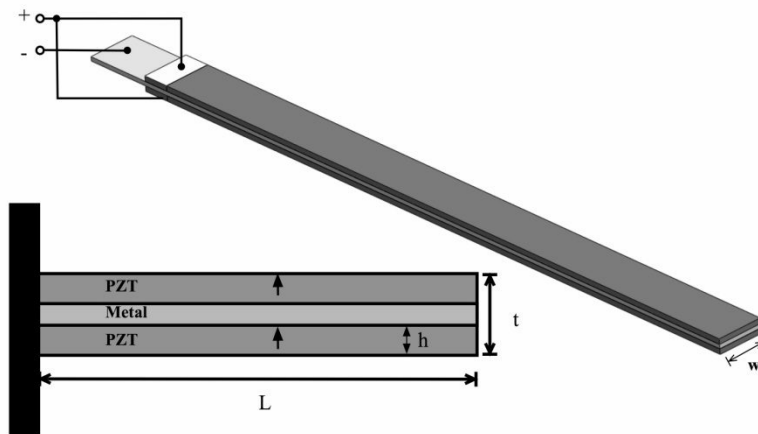


**Figure 1:** A schematic diagram of piezoelectric bimorph in parallel connection.

$$\begin{pmatrix} \alpha \\ \delta \\ v \\ Q \end{pmatrix} = \begin{pmatrix} \frac{3s_{11}^E L}{2wh^3} & \frac{3s_{11}^E L^2}{4wh^3} & \frac{s_{11}^E L^3}{4h^3} & \frac{-3d_{31}L}{2h^2} \\ \frac{3s_{11}^E L^2}{4wh^3} & \frac{s_{11}^E L^3}{2wh^3} & \frac{3s_{11}^E L^4}{16h^3} & \frac{-3d_{31}L^2}{4h^2} \\ \frac{s_{11}^E L^3}{4h^3} & \frac{3s_{11}^E L^4}{16h^3} & \frac{3ws_{11}^E L^5}{40h^3} & \frac{-d_{31}wL^3}{4h^2} \\ \frac{-3d_{31}L}{2h^2} & \frac{-3d_{31}L^2}{4h^2} & \frac{-d_{31}wL^3}{4h^2} & \frac{2\varepsilon_{33}^T wL}{h} \left(1 - \frac{k_{31}^2}{4}\right) \end{pmatrix} \begin{pmatrix} M \\ F \\ p \\ V \end{pmatrix} \quad (2)$$

where  $d_{31}$ ,  $k_{31}$  and  $s_{11}^E$  are the piezoelectric strain coefficient, electromechanical coupling and open circuit elastic compliance, respectively.  $\varepsilon_{33}^T$  is the dielectric permittivity.  $L$ ,  $w$ , and  $h$  are length, width, and thickness of a piezoelectric element. If only an external force  $F$  is acting at the bimorph tip under an open circuit condition, the tip deflection, generated electrical charge and voltage can be calculated using the following equations (3-5), which allows for the calculation of the amount of the electrical energy ( $E=1/2 QV$ ) converted from mechanical force ( $F$ ) for a given piezoelectric material.

$$\delta = \frac{4s_{11}^E L^3}{wt^3} * F \quad (3)$$

$$Q_{oc} = \frac{3d_{31}L^2}{4h^2} * F \quad (4)$$

$$V_{oc} = \frac{3g_{31}L}{8wh} * F \quad (5)$$

where  $t$  is the total thickness of the bimorph and  $g_{31}$  is the piezoelectric voltage coefficient. This highlights that the generated electrical energy is proportional to the product of piezoelectric  $d$  and  $g$  coefficients.

A piezoelectric harvester generates the maximum power when it is made to vibrate at its resonant frequency. Thus, the key requirement for the harvester design is to match the frequency content of the unsteady flow to the resonance frequency of the vibrating structure in a closely coupled fluid-structure interaction design. The induced vibration frequency of a cantilever in a fluid flow is expected to be in the low frequency regime (i.e.,  $< 1$  kHz), requiring a low resonant frequency bimorph structure. The natural frequency of the bimorph can be predicted using the following equation (6)[21].

$$\omega_r = \frac{t}{L^2} \sqrt{\frac{1}{\rho s_{11}^E}} \quad (6)$$

A piezoelectric bimorph in a parallel connection produced by APC International[22] was used to demonstrate the power generation in a proof-of-concept flow energy harvester. This bimorph consists of two thin (0.2 mm) strips of piezoelectric elements that are 44 mm long (free length) and 2 mm wide. They are covered with a thin layer to protect and electrically isolate the electrodes. The physical and electrical parameters of this bimorph are listed in Table 1.

Finite element analysis of the bimorph harvester was performed to investigate the power output capability of this bimorph design. In this model, the bimorph transducer was surrounded by air, and the electrical impedance was simulated using circuit models. Experimental electrical impedance of this bimorph was also determined using a network analyzer (HP 4294A, Hewlett Packard, Palo Alto, CA). The simulated electrical impedance from the bimorph mounted in harvester over a frequency range (40-1200 Hz) is shown in Figure 2. For comparison, the measured electrical impedance with the HP 4294A network is also plotted. Note that the simulated impedances were close to those from the measured HP

4294A network. The measured first mode natural resonance frequency and the second harmonic of the bimorph are found to be 160 Hz, and 1018 Hz, respectively, while those from simulated results are 165 Hz and 1050 Hz, respectively.

**Table 1: Dimension and electrical properties for the piezoelectric bimorph.**

	$\rho$ (kg/m <sup>3</sup> )	Y (GPa)	L (mm)	w (mm)	h (mm)	$\epsilon_{33}^T/\epsilon_0$	$d_{31}$ (pC/N)	$S_{11}^E$ (pm/N)
PZT	7500		44	2	0.2	3400	274	16.5
Brass	8300	115	49	2	0.25			

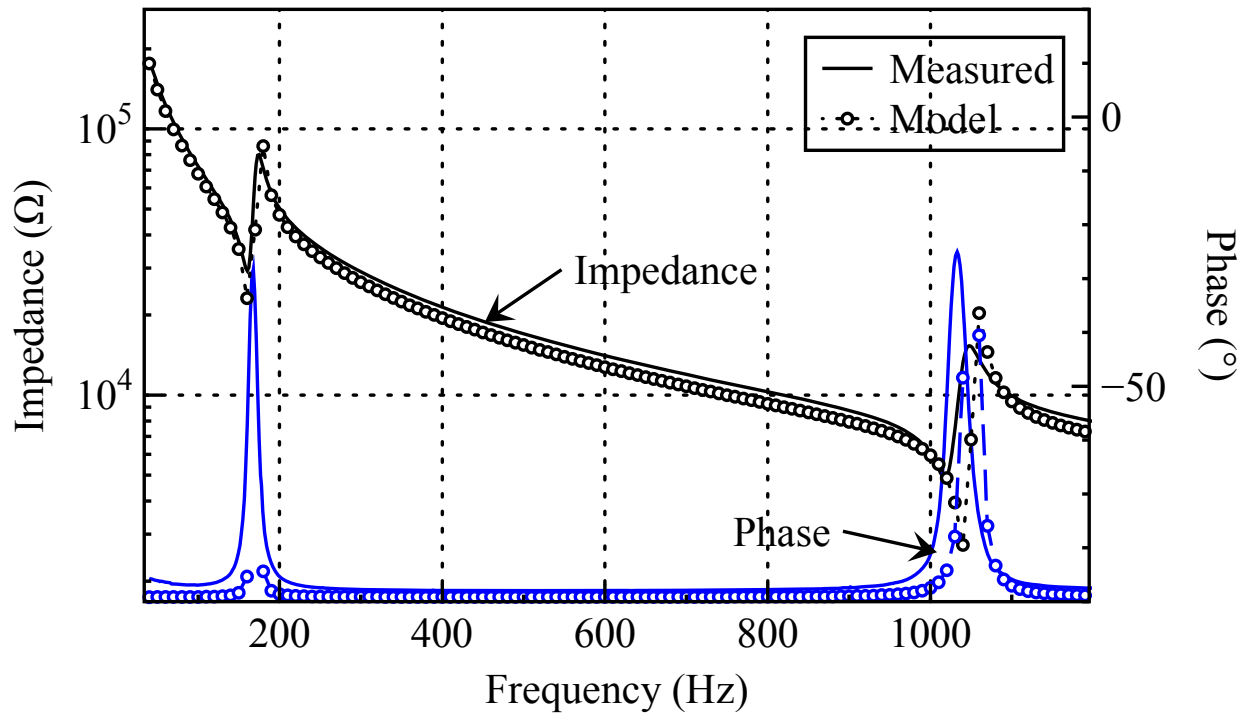


**Figure 2:** Impedance and phase spectra of bimorph mounted in the harvester chamber (fixed-free).

Note that in order to achieve maximum power transfer from the source to the load, the load resistance is matched to the source impedance (piezoelectrics). The optimum electrical impedance of piezoelectric material can be calculated by  $1/j\omega C + R$ , where  $R$  and  $C$  are the internal resistance and capacitance related to the dielectric permittivity and loss (i.e.,  $R = \tan\delta/\omega C$ ) of the piezoelectric material[23]. Figure 3 shows the theoretical power output as a function of frequency and load resistance. In the frequency-resistance plane from simulated results, the magnitude of normalized power level was represented by contour. In the calculation, it was assumed that the applied force  $F$  is 0.1 N, which gives approximately 0.8 mm deflection according to the equation (5). As expected, a large output power can be obtained at both resonant (160 kHz) and antiresonant (170 kHz) frequencies at the matched impedances, being on the order of 0.5-0.6 mW. This indicates that the piezoelectric bimorph is capable of generating power in the milliwatt range under 1 mm tip deflection.

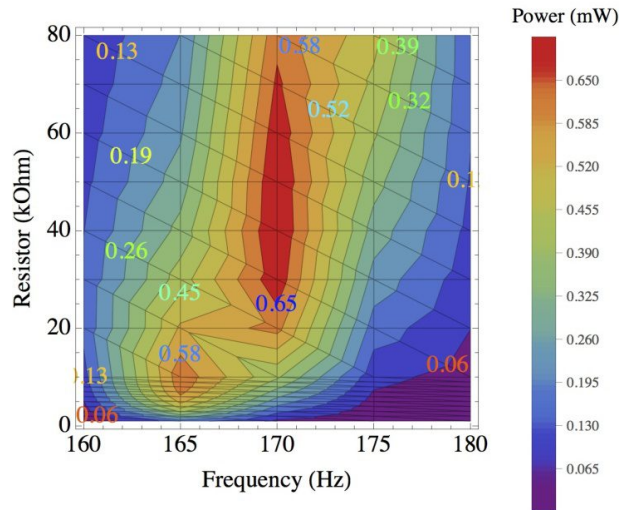


**Figure 3:** Theoretical power output as a function of load resistance and drive frequency under 0.1 N force on the tip of the bimorph.

### III. Flow energy harvester design and tests

There are a variety of potential methods to couple the flow energy to the structure with the transduction mechanism located away from the flow. Several types of flow induced energy harvester methods were considered in this study; one is a hydraulic pressure based method[18, 24], a second is a bluff body based method[12,13,14,15,16], yet another is based on leakage-flow instabilities which induce large displacements in the bimorph tip when fluid flows past a narrow passage [25]. For example, when the flow is passing through the nozzle, the pressure fluctuation forces the bimorph to move alternately up and down, creating internal stresses and producing electricity. The asymmetric pressure distribution on the surface of the piezoelectric bimorph results in the oscillatory deflection and the generation of electrical power. Schematic drawings of a few of these models and designs are shown in Figure 4.

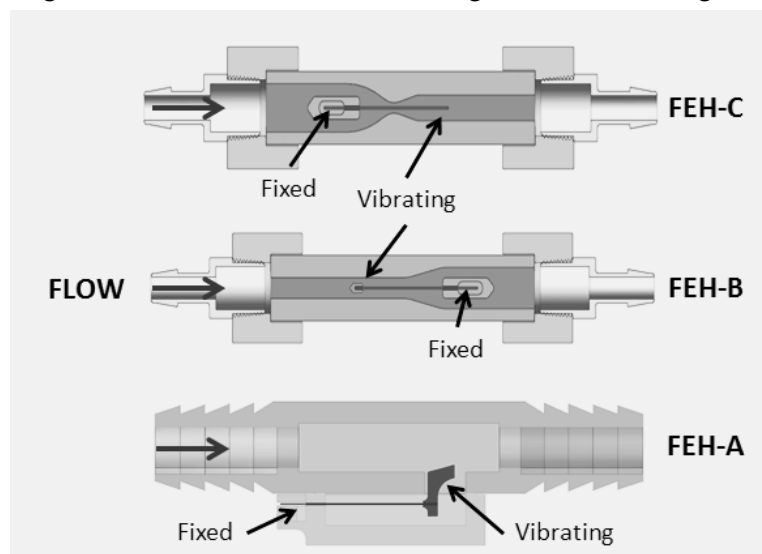


**Figure 4:** Model and schematic diagrams of flow energy harvester designs. The driving force of FEH-A design is the fluid pressure fluctuation, while that of FEH-B (straight profile) are flow instabilities associated with slender structures in axial flow (leakage-flows) and C (spline profile) a combination of leakage, diffuser, and tip-vortex shedding flow instabilities.

The preliminary measurements on each harvester was performed to characterize the flow nozzle design. A series of flow channels, including those in Figure 4, were manufactured by rapid prototyping using clear SLA materials cross section [26]. The initial measurements were made using the water pressure in the lab and opening to atmospheric pressure. During tests, the flow rate was adjusted and the power generated from the nozzle was monitored across an adjustable resistance using a digital oscilloscope (Model Tektronix TDS5054B-NV). A schematic of the experimental set up is shown in Figure 5. A labview program was written to monitor the voltage waveform across the load resistor as a function of time and to calculate the average power. The program also displayed the voltage frequency content by displaying the Fast Fourier Transform (FFT) of the voltage waveform.

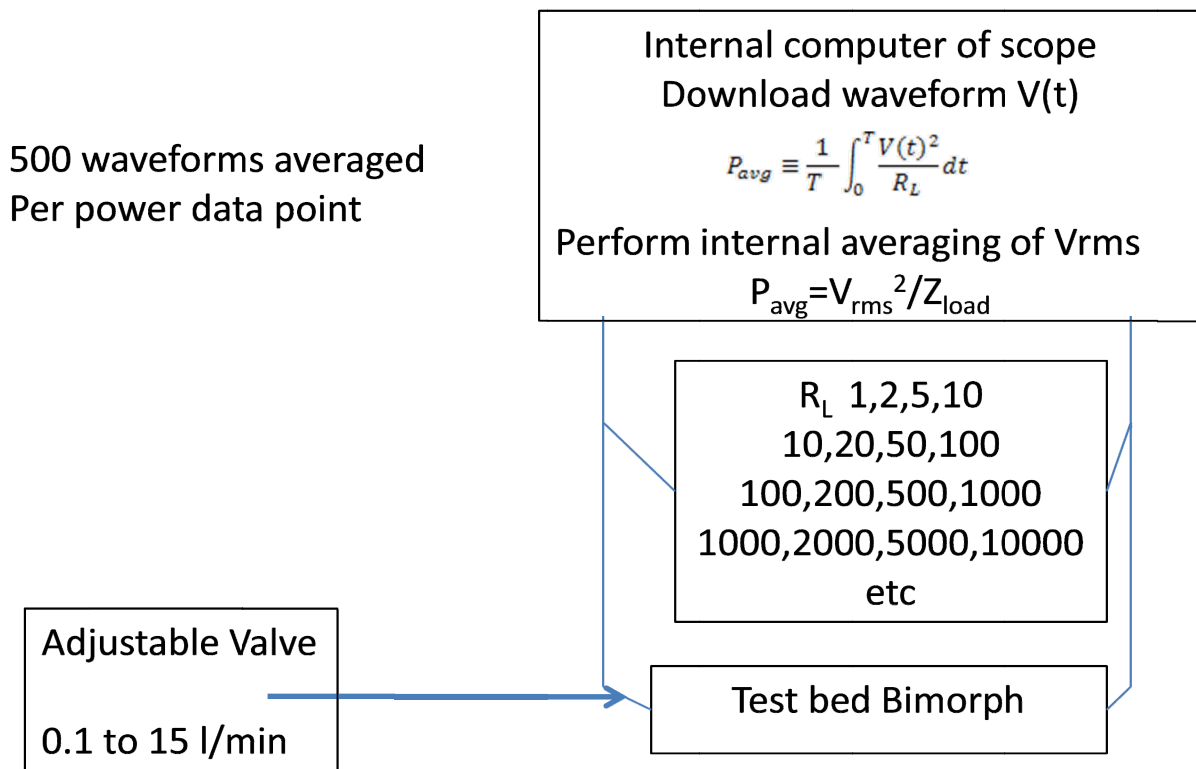


**Figure 5:** A schematic of the experimental setup used to test the flow energy harvesters.

It is interesting to note that during the test, the frequency contents of output voltages from the flowing media were found to be broadband, exciting the bimorph over a range of frequencies that encompass the first and second resonances depending on the load resistance. Figure 6 shows the examples of waveforms of the output voltage and Fast Fourier Transform (FFT) of the received signals from the spline nozzle design (FEH-C) when 10 kOhm and 50 kOhm are connected as a load. Note that in the frequency domain with the harvester connected to a relatively low resistor (10 kOhm), the FFT showed high intensity peaks at both first and second resonant frequency. However, when the harvester was connected to the 50 kOhm resistor, most energy was concentrated around the fundamental resonant frequency of the bimorph (150 Hz). It also had a larger output voltage.

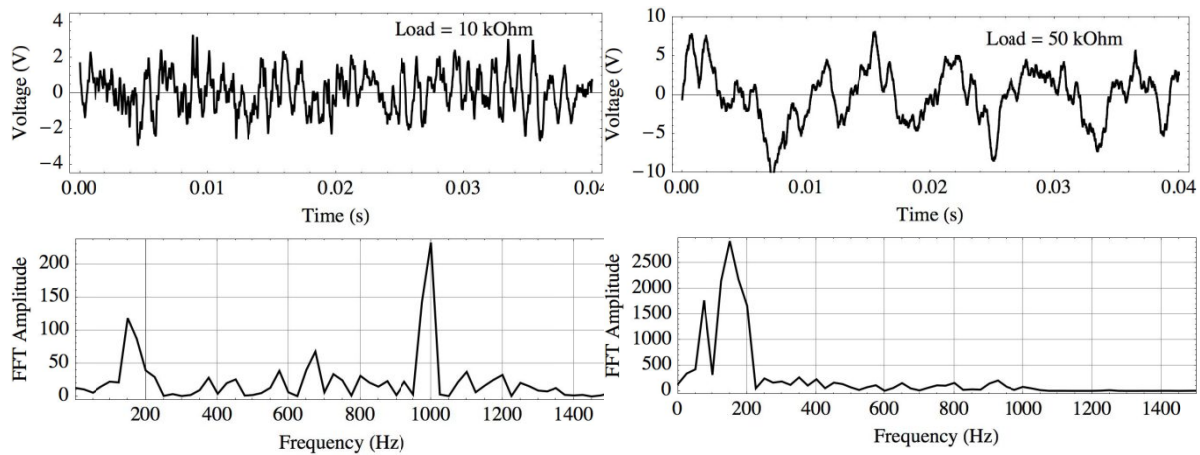


**Figure 6:** Time domain signal and Fast Fourier Transform (FFT) of FEH-C (spline profile) bimorph harvester under a flow rate of 10 L/min when a 10 kOhm (left) and 50 kOhm (right) resistor is connected as a load.

The power output as a function of the load resistance for the prototype harvesters is shown in Figure 7 under a flow rate of 10 L/min. In general, it was found that the nozzle designs FEH-B and C produced an order of magnitude higher power output levels than FEH-A harvester. The instabilities driving the bimorph arise from a combination of unsteadiness in the nozzle itself (enhanced by the moving bimorph) and the bimorph tip vortices that shed from the boundary layer at the top and bottom of the cantilever. The maximum power output of FEH-A is found to be on the order of 0.04 mW, while those of FEH-B and FEH-C are 0.1 mW and 0.54 mW, respectively. The optimum load of each design is found to be 50 kOhm, which is close to the impedance at the first resonance frequency of the bimorph in water.

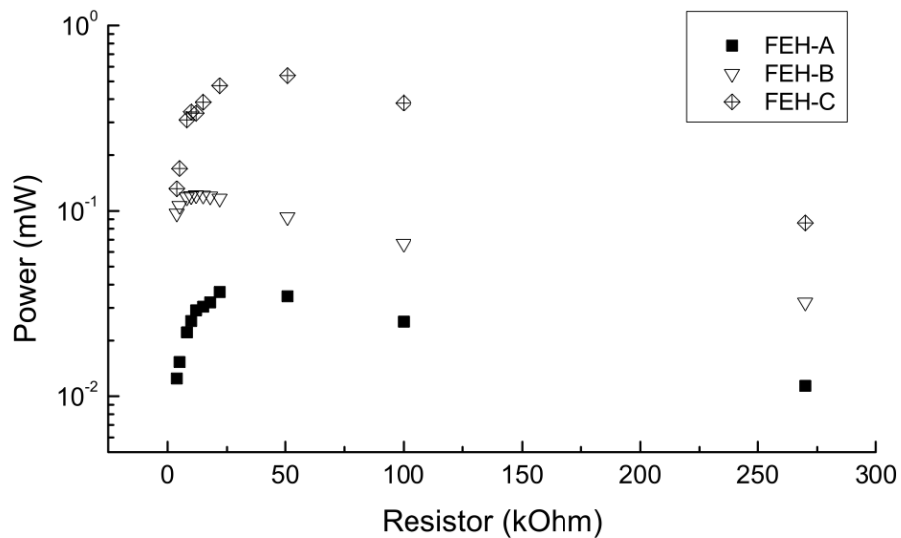


**Figure 7:** Power output of various nozzle designs as a function of the load resistance.

Due to the superior performance of FEH-C nozzle design over the other harvesters, further analysis was performed using this design. One of the concerns for nozzle design of FEH-C was the noticeable cavitation after the expansion in the neck of the nozzle which is known to be suppressed under high pressure. In order to remove cavitation as a possible source of the flow structure coupling, a higher pressure test loop was designed and built that maintained a nominal pressure at the outlet to inhibit

cavitation. A photograph of the flow loop is shown in Figure 8. The loop contains a motor/ pump, a reservoir, a regulator and a pressure gauge before and after the flow energy harvester, a filter, a safety release valve and a flow meter. The pressure before and after the flow energy harvester is measured and controlled by the pump current and needle valve to the harvester, and the flow rate is monitored using flow meters. The flow loop output is collected into an open reservoir and the pump draws the fluid from the bottom of this reservoir.

The initial rapid prototype harvesters were not designed to withstand the larger pressures. During testing, there were leaks in the plexi-glass plate at the glue joint. In order to accommodate the higher pressure the harvesters were also redesigned, where the flow profile is mounted on the body of the harvester and an o-ring is inserted into the groove. The plexi-glass cover is screwed into it to seal against the o-ring. A schematic diagram of this design is shown in the inset in Figure 8.

The results of the test for the FEH-C design depending on the load resistance and flow rate are listed in Table 2. Note that when the flow rate is low, no deformation on the bimorph occurred, producing negligible voltage output. This is because the instantaneous pressure distribution over the length of the bimorph is largely symmetric about its length. A noticeable voltage or power output was found when the flow rate exceeded 3 L/min. Above this level the power level increased with increasing flow rate. The power was measured to be 0.5 mW under a flow rate of 3.8 L/min and jumped to 3.5 mW under a flow rate of 7.6 L/min. The maximum average power levels were found at matched resistances that ranged between 20 kOhms for the lower flow levels and 50 kOhm for the higher flow rates.



**Figure 8:** A photograph of closed flow loop system. The inset shows a schematic diagram of a spline nozzle harvester design.

An example of the output voltage waveform and FFT analysis under 5.6 L/min with a 20 kOhm load resistor is shown in Figure 9. Note that in the frequency domain, most of the energy was concentrated at the first resonant frequency with a relatively narrow band compared to the frequency response of previous nozzle design shown in Figure 6. The tip deflections of the bimorph were in the range from 2 and 3 mm. Interestingly, a further increase in flow rate above 7.7 L/min resulted in a mode change from the first mode to second harmonic mode, exhibiting a second harmonic deflection with high frequency excitations in the 500-600 Hz range. The power level was observed to be essentially flat with flow rate above 7.7 L/min.

**Table 2: Generated electrical power for new flow harvester design. SD=standard deviation**

Flow Rate (L/min)	R (kOhm)	$P_{\min}$ (mW)	$P_{\max}$ (mW)	$P_{\text{avg}}$ (mW)	SD
3.8	20	0.23	0.37	0.31	0.03
	40	0.24	0.49	0.36	0.05
	50	0.29	0.47	0.39	0.04
7.6	20	2.41	3.35	2.87	0.16
	30	2.31	3.18	2.86	0.23

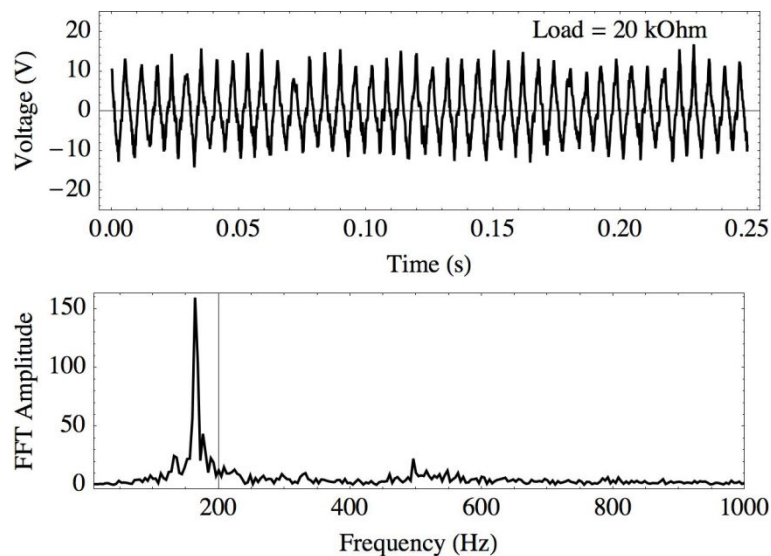


**Figure 9:** Time domain signal and Fast Fourier Transform (FFT) of bimorph harvester.

#### IV. Conclusion and Future work

Flow energy piezoelectric harvesters were investigated, and it was found that spline nozzle design showed superior performance over other nozzle designs, generating upto 3.5 mW at a matched resistance. The ability to generate 3.5 mW showed that these materials when arrayed may be capable of generating average powers at or approaching levels required by the application. In addition it demonstrated that by controlling flow rate it is possible to couple flow energy to structures at the levels required. It was noted however, that under extended use the bimorph was damaged due to impacts of the bimorph on the throat of the spline nozzle, and its performance decreased. In addition when driven at high flow rates, the strain in the bimorph exceeded the ultimate strain and cracks formed causing a reduction in life as well as a power degradation. In order to solve this issue, new transducer designs are currently being investigated, where a non piezoelectric cantilever is fixed between two piezoelectric transducers.

## ACKNOWLEDGMENT

The research at the Jet Propulsion Laboratory (JPL), a division of the California Institute of Technology, was carried out under a contract with the National Aeronautics Space Agency (NASA). Reference herein to any specific commercial product, process, or service by trade name, trademark, manufacturer, or otherwise, does not constitute or imply its endorsement by the United States Government or the Jet Propulsion Laboratory, California Institute of Technology.

## REFERENCES

- [1] S. Sherrit, "The physical acoustics of energy harvesting," Proceedings of the IEEE Ultrasonics Symposium -IUS 2008, 1046–1055 , ( 2008)
- [2] S. Priya, "Advances in energy harvesting using low profile piezoelectric transducers," Journal of Electroceramics, vol. 19, no. 1, pp. 167–184, (2007)
- [3] N. S. Shenck, "A demonstration of useful electric energy generation from piezoceramics in a shoe," Ph.D. dissertation, Massachusetts Institute of Technology, Dept. of Electrical Engineering and Computer Science, (1999)
- [4] J. A. Paradiso and T. Starner, "Energy scavenging for mobile and wireless electronics," Pervasive Computing, IEEE, vol. 4, no. 1, pp. 18–27, (2005)
- [5] S. R. Platt, S. Farritor, and H. Haider, "On low-frequency electric power generation with pzt ceramics," Mechatronics, IEEE/ASME Transactions on, vol. 10, no. 2, pp. 240–252, (2005)
- [6] M. Lallart, L. Garbuio, L. Petit, C. Richard, and D. Guyomar, "Double synchronized switch harvesting (dssh): a new energy harvesting scheme for efficient energy extraction," Ultrasonics, Ferroelectrics and Frequency Control, IEEE Transactions on, vol. 55, no. 10, pp. 2119–2130, (2008)
- [7] N. S. Shenck and J. A. Paradiso, "Energy scavenging with shoe-mounted piezoelectrics," Micro, IEEE, vol. 21-no. 3, 30–42, (2001)
- [8] D. Guyomar, A. Badel, E. Lefeuvre, and C. Richard, "Toward energy harvesting using active materials and conversion improvement by nonlinear processing," , IEEE Transactions on Ultrasonics, Ferroelectrics and Frequency Control, vol. 52-no. 4, 584–595, (2005)
- [9] A. Soma and G. De Pasquale, "Design of high-efficiency vibration energy harvesters and experimental functional tests for improving bandwidth and tunability," SPIE Microtechnologies, U. Schmid, J. L. S´anchez de Rojas Aldavero, and M. Leester-Schaedel, Eds. SPIE, 87630U. , (2013)
- [10] J. Dias, C. De Marqui, and A. Erturk, "Electroaeroelastic modeling and analysis of a hybrid piezoelectric-inductive flow energy harvester," Proceedings of SPIE Smart Structures and Materials+ Nondestructive Evaluation and Health Monitoring. International Society for Optics and Photonics, 86 882N–86 882N, (2013)
- [11] D. Zhu, Vibration Energy Harvesting: Machinery Vibration, Human Movement and Flow Induced Vibration, (2011)
- [12] J. J. Allen and A. J. Smits, "Energy Harvesting Eel," Journal of Fluids and Structures, vol. 15- no. 3-4, 629–640, (2001)
- [13] E. Bischur, S. Pobering, M. Menacher, and N. Schwesinger, "Piezoelectric energy harvester operating in flowing water," Proc. of SPIE , vol. 7643, 76 432Z–1, ( 2010)

- [14] X. Gao, W.-H. Shih, and W. Y. Shih, "Flow Energy Harvesting Using Piezoelectric Cantilevers With Cylindrical Extension," *IEEE Transactions on Industrial Electronics*, vol. 60- no. 3, 1116–1118, (2013)
- [15] E. Molino-Minero-Re, M. Carbonell-Ventura, C. Fisac-Fuentes, A. Manuel-Lazaro, and D. M. Toma, "Piezoelectric energy harvesting from induced vortex in water flow," *Proceedings of the IEEE International Instrumentation and Measurement Technology Conference (I2MTC)*, 624–627, (2012)
- [16] J. D. Hobeck and D. J. Inman, "Electromechanical and statistical modeling of turbulence-induced vibration for energy harvesting," *Proceedings of the SPIE Smart Structures and Materials+ Nondestructive Evaluation and Health Monitoring* , 86 881P, (2013)
- [17] M. Bryant, M. W. Shafer, and E. Garcia, "Power and efficiency analysis of a flapping wing wind energy harvester", *Proceedings of the SPIE Smart Structures and Materials+ Nondestructive Evaluation and Health Monitoring*. 83410E, (2012)
- [18] E. A. Skow, K. A. Cunefare, and A. Erturk, "Design and performance enhancement of hydraulic pressure energy harvesting systems," *Proceedings of the SPIE Smart Structures and Materials+ Nondestructive Evaluation and Health Monitoring*, 868803, (2013)
- [19] J. G. Smits and W.-s. Choi, "The constituent equations of piezoelectric heterogeneous bimorphs", *IEEE transactions on ultrasonics, ferroelectrics, and frequency control*, vol. 38- no. 3, 256–270, (1991)
- [20] J. G. Smits and A. Ballato, "Dynamic behavior of piezoelectric bimorphs," *Proceedings of the IEEE International Ultrasonics Symposium*,. 463–465, (1993)
- [21] K. Uchino, *Ferroelectric devices*., New York, NY: Marcel Dekker, Inc., vol. 16, (2000)
- [22] APC International Ltd., Model #'s 40-1025, 40-1035, see [<https://www.americanpiezo.com/standard-products/stripe-actuators.html>], (2013)
- [23] H. Kim, S. Priya, and K. Uchino, "Modeling of Piezoelectric Energy Harvesting Using Cymbal Transducers," *Japanese Journal of Applied Physics*, vol. 45- no. 7, 5836–5840, ( 2006)
- [24] G. Ye and K. Soga, "Energy Harvesting from Water Distribution Systems," *Journal of Energy Engineering*, vol. 138- no. 1, 7–17, (2012)
- [25] M. P. Paidossis., "Annular- and Leakage- Flow-Induced Instabilities," *Fluid-Structure Interactions: Slender Structures and Axial Flow*, Volume 2, Academic Press, 1221–1420, (2003)
- [26] Solid Concepts Inc. , "3D Printing & Rapid Prototyping Services", [[www.solidconcepts.com](http://www.solidconcepts.com)], (2013)